Recognition of Heptoses and the Inner Core of Bacterial Lipopolysaccharides by Surfactant Protein D†

Hua Wang,‡ James Head,‡ Paul Kosma,§ Helmut Brade,|| Sven Müller-Loennies,|| Sharmin Sheikh,⊥ Barbara McDonald,⊥ Kelly Smith,⊥ Tanya Cafarella,‡ Barbara Seaton,‡ and Erika Crouch*,⊥

Department Physiology and Biophysics, Boston University School of Medicine, Boston, Massachusetts 02118, Department of Chemistry, University of Natural Resources and Applied Life Sciences, Vienna, Austria, Department of Immunochemistry and Biochemical Microbiology, Leibniz Center for Medicine and Biosciences, D-23845 Borstel, Germany, and Department of Pathology and Immunology, Washington University School of Medicine, St. Louis, Missouri 63110

Received October 12, 2007

ABSTRACT: Lipopolysaccharides (LPS) of Gram-negative bacteria are important mediators of bacterial virulence that can elicit potent endotoxic effects. Surfactant protein D (SP-D) shows specific interactions with LPS, both in vitro and in vivo. These interactions involve binding of the carbohydrate recognition domain (CRD) to LPS oligosaccharides (OS); however, little is known about the mechanisms of LPS recognition. Recombinant neck+CRDs (NCRDs) provide an opportunity to directly correlate binding interactions with a crystallographic analysis of the binding mechanism. In these studies, we examined the interactions of wild-type and mutant trimeric NCRDs with rough LPS (R-LPS). Although rat NCRDs bound more efficiently than human NCRDs to *Escherichia coli* J-5 LPS, both proteins exhibited efficient binding to solid-phase Rd2-LPS and to Rd2-LPS aggregates presented in the solution phase. Involvement of residues flanking calcium at the sugar binding site was demonstrated by reciprocal exchange of lysine and arginine at position 343 of rat and human CRDs. The lectin activity of hNCRDs was inhibited by specific heptoses, including L-*glycero*-α-D-*manno*-heptose (L,D-heptose), but not by 3-deoxy-α-D-*manno*-oct-2-ulosonic acid (Kdo). Crystallographic analysis of the hNCRD demonstrated a novel binding orientation for L,D-heptose, involving the hydroxyl groups of the side chain. Similar binding was observed for a synthetic α1→3-linked heptose disaccharide corresponding to heptoses I and II of the inner core region in many LPS. 7-*O*-Carbamoyl-L,D-heptose and D-*glycero*-α-D-*manno*-heptose were bound via ring hydroxyl groups. Interactions with the side chain of inner core heptoses provide a potential mechanism for the recognition of diverse types of LPS by SP-D.

Lipopolysaccharides are critical structural components of the Gram-negative cell wall and play important roles in bacterial virulence (*1*). The release of LPS[1] (endotoxin) elicits a wide variety of inflammatory responses that contribute to the development of shock and other manifestations of Gram-negative sepsis. The overall structure of LPS is well-conserved among Gram-negative organisms and always consists of a lipid A domain and a core oligosaccharide and, in many bacteria, of a terminal O-polysaccharide (O-PS) (*1*, *2*). Whereas the O-PS consists of repeating saccharide units of variable length and composition and thus exhibits a high degree of structural variability, the core oligosaccharide (OS) is highly conserved. The inner core contains Kdo (3-deoxy-α-D-*manno*-oct-2-ulosonic acid) and heptose, usually L-*glycero*-α-D-*manno*-heptose (L,D-heptose), but sometimes D-*glycero*-α-D-*manno*-heptose (D,D-heptose). The inner core sugars are susceptible to variable modification by substitution with phosphate (*P*), phosphorylethanolamine (*P*Etn), pyrophosphorylethanolamine (*PP*Etn), or other sugars (*3*).

Surfactant protein D (SP-D), a collagenous C-type lectin or collectin, plays important roles in the innate immune host response to a wide variety of microorganisms (*4*−*8*). Although most abundant in lung, SP-D is expressed at many mucosal sites, including the gastrointestinal and genitourinary tracts. In general, SP-D's microbial interactions involve the specific recognition of surface glycoconjugates. As for other "mannose-type" C-type lectins, carbohydrate binding is primarily mediated by interactions of the vicinal hydroxyl groups at positions 3 and 4 of the carbohydrate ring with a calcium ion, here termed Ca1, and further stabilized by contacts with residues that coordinate with this ion (*9*−*12*). Depending on the lectin, ligand recognition can involve one or more sites of secondary interaction with the CRD.

† This work was supported by National Institutes of Health Grants HL-44015 and HL-29594 (E.C.) and by the Deutsche Forschungsgemeinschaft (SFB470/C1).

* To whom correspondence should be addressed: Department of Pathology and Immunology, Campus Box 8118, Washington University School of Medicine, 660 S. Euclid Ave., St. Louis, MO 63110. Telephone: (314)454-8462. Fax: (314)454-5917. E-mail: crouch@path.wustl.edu.

‡ Boston University School of Medicine.

§ University of Natural Resources and Applied Life Sciences.

|| Leibniz Center for Medicine and Biosciences.

⊥ Washington University School of Medicine.

[1] Abbreviations: BSA, bovine serum albumin; LPS, lipopolysaccharide; SP-D, surfactant protein D; CRD, carbohydrate recognition domain; NCRD, trimeric neck+CRD; L,D-heptose or L,D-Hep, L-*glycero*-α-D-*manno*-heptose; D,D-heptose or D,D-Hep, D-*glycero*-α-D-*manno*-heptose; 2-deoxyheptose, 2-deoxy-L-*galacto*-heptose; Kdo, 3-deoxy-α-D-*manno*-oct-2-ulosonic acid.

10.1021/bi7020553 CCC: $40.75
Published on Web 12/20/2007

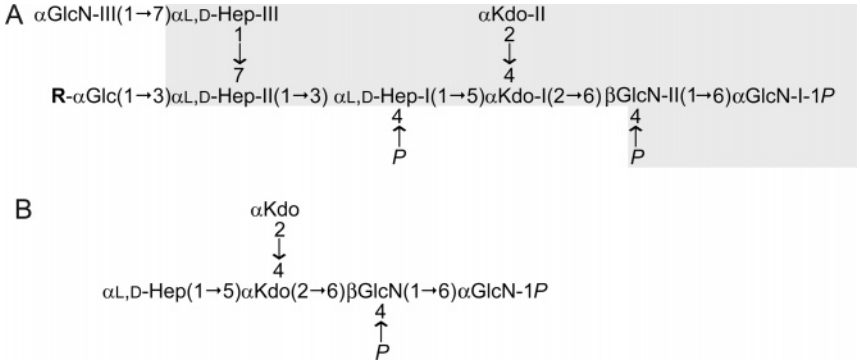

FIGURE 1: LPS core oligosaccharides. (A) Chemical structure of a nonasaccharide trisphosphate as obtained after deacylation of *E. coli* J-5 LPS. R designates the outer core region in strains with a more complete core oligosaccharide; glucose is exposed in the intact J-5 LPS and purified nonasaccharide trisphosphate. Note that Hep-II can be substituted at position 4 with phosphorus when the side chain heptose residue is not substituted with GlcN-III. Areas of structure demarcated in gray are shared with many LPS of Gram-negative bacteria but vary in the degree of phosphorylation and other modifications. (B) Pentasaccharide bisphosphate carbohydrate backbone as present in Rd2 chemotype LPS, occurring in core-defective mutants that lack the phosphorylation of the heptose residue.

Gram-negative LPS was the first microbial ligand shown to be recognized by SP-D, and interactions with LPS were the first to suggest host defense functions for surfactant-associated proteins (*13*). The binding of SP-D to LPS involves interactions of the carbohydrate recognition domain (CRD) of SP-D with the core OS and/or PS chains of LPS (*14*). Although SP-D can bind to specific O-PS on certain "smooth" strains (*15*), SP-D generally prefers rough LPS (*13*, *16*, *17*), and recognition appears to preferentially involve interactions with the core (*13*). However, the mechanism of core interaction has not been characterized.

Recognition of LPS has been implicated in the SP-D-dependent agglutination and/or internalization and killing of certain Gram-negative bacteria by macrophages (*17*, *18*). SP-D can bind or agglutinate specific strains derived from a wide variety of Gram-negative species, including such important pathogens as *Pseudomonas aeruginosa* (*18*−*20*), *Klebsiella pneumoniae* (*17*), *Escherichia coli* (*13*, *16*), *Bordetella pertussis* (*21*), *Haemophilus influenzae* (*22*), and *Helicobacter pylori* (*23*). In addition, interactions of SP-D can mediate direct bactericidal effects on rough bacteria, probably through binding to LPS with associated perturbations in membrane permeability (*24*). The in vitro data are consistent with bacterial challenge experiments using SP-D deficient mice. These animals exhibit a decreased level of internalization of Gram-negative bacteria by macrophages (*22*), impaired clearance and an increased level of dissemination of non-mucoid *P. aeruginosa* (*20*), and enhanced colonization and altered immune responses to *Helicobacter* (*25*). There is also evidence that SP-D can modulate the response to purified endotoxin in vivo (*26*−*28*). Although some effects could involve modulation of the phagocyte response to LPS (*29*), the available data strongly suggest that SP-D contributes to endotoxin neutralization through direct interactions with the bacterial lipopolysaccharides.

SP-D is secreted as multimers of trimeric subunits with C-terminal lectin domains (*30*). Trimerization of the carbohydrate recognition domains (CRDs) is required for high-affinity ligand binding, and this structure is maintained by the neck domain. The trimeric recombinant neck+CRD (NCRD) demonstrates many, if not most, of the activities of the intact molecule, in vitro and in vivo (*31*, *32*). Unlike the native molecule, NCRDs are also ideally suited to structural analysis of their binding mechanism via crystallography and other biophysical techniques (*11*, *12*). This prompted an examination of LPS recognition using trimeric NCRDs and purified subdomains of the LPS core oligosaccharide.

EXPERIMENTAL PROCEDURES

The pET-30a(+) vector, S-protein horseradish peroxidase (S-protein HRP), and RosettaBlue competent cells were from Novagen (Madison, WI). Fatty acid-free BSA with low immunoglobulin (BAH66-0050) was from Equitech-Bio, Inc. (Kerrville, TX). *E. coli* J-5 LPS (Rc chemotype) and the Re-LPS from *Salmonella enterica* sv. Minnesota were from List Biological Laboratories; however, for some initial experiments, nominally equivalent preparations were obtained from Sigma-Aldrich (St. Louis, MO). *E. coli* F583 Rd2-LPS, *E. coli* O111:B4 LPS, yeast mannan, maltosyl-BSA, oxidized and reduced glutathione, and competing sugars were also from Sigma-Aldrich. All mono- and disaccharides were the α-D-anomers and of the highest purity available.

The nonasaccharide trisphosphate αGlc(1→3)[αGlcN-(1→7)αHep(1→7)]αHep(1→3)αHep4*P*(1→5)[αKdo-(2→4)]αKdo(2→6)*β*GlcN4*P*(1→6)αGlcN1*P* (Figure 1A) was isolated from *E. coli* J-5 LPS after deacylation and separated by high-performance anion exchange chromatography (Dionex) as reported previously (*33*, *34*); it was conjugated to bovine serum albumin (BSA) by the glutardialdehyde method as described previously (*35*).

Heptose Synthesis and Characterization. L,D-Heptose and D,D-heptose were synthesized according to the method described by Brimacombe (*36*). The heptose disaccharide and the 7-*O*-carbamoylheptose were synthesized according to published procedures (*37*, *38*). The D-*glycero*-D-*manno*-heptose 7-phosphate was prepared via the phosphoramidite method (*39*), and 2-deoxy-L-*galacto*-heptose was prepared via indium-promoted chain elongation of L-lyxose (*40*). Ammonium Kdo was prepared via the Cornforth reaction. The purity and identity of the ligands were confirmed by 300 MHz ^{1}H NMR spectroscopy; the purity was >95%.

Generation of Fusion Constructs. Constructs encoding N-terminally tagged, trimeric human and rat neck+CRD fusion proteins (hNCRD and rNCRD, respectively) were

generated using the pET30a(+) vector system as previously described (*31*, *41*). All NCRDs are cloned into the BamHI−HindIII sites of the vector, providing N-terminal His tags, an S-protein binding site, and an enterokinase cleavage site. Mutant NCRD constructs included human R343K, human R343A, and rat K343R (*12*), as well as human D325N (*41*).

Constructs encoding tagless hNCRDs were generated via re-engineering of the expression plasmid to delete the entirety of the fusion tag and place the first residue of the natural neck domain C-terminal to the initiator methionine. The pET30a(+) vector contains a NdeI site immediately preceding the His tag coding sequence. Mutagenesis of BamHI to NdeI allowed excision of the entirety of the fusion tag with NdeI. The modified vector was gel repurified and religated with T4 ligase prior to bacterial transformation and DNA sequencing.

Isolation of Trimeric Neck+CRD Domains. RosettaBlue competent cells were transformed with the desired plasmid and induced (*31, 41*). Fusion proteins were then extracted from exclusion bodies and refolded as previously described, except that inclusion bodies were solubilized using 6 M guanidine hydrochloride and 50 mM Tris-HCl (pH 7.5) containing 5 mM dithiothreitol. In addition, the refolding buffer was supplemented with 5 mM reduced and 0.5 mM oxidized glutathione to facilitate disulfide exchange. Refolded proteins were purified by chelation chromatography, and trimers were isolated by gel filtration chromatography on Superose 12 in the absence of calcium (*31, 41*).

For crystallographic studies, neck+CRDs were generated by enterokinase cleavage of the fusion proteins (*11*, *12*), or by expression of NCRDs lacking the fusion tags. At the completion of refolding, the tagless NCRDs were dialyzed versus 150 mM NaCl and 10 mM Hepes (pH 7.5) containing 10 mM calcium chloride (HBSC) and purified by maltosyl-agarose chromatography (*41*); trimers were then isolated by gel filtration chromatography in HBSC (*11*). The major peak, corresponding to the trimer, was pooled, and the protein was concentrated by ultrafiltration to approximately 15 mg/mL prior to being frozen at −80 °C.

All proteins migrated as a single major band via SDS−PAGE and migrated more slowly upon being reduced, consistent with normal folding of the intrachain disulfide bonds (*31*, *41*) (data not shown). Endotoxin was routinely quantified using a QCl-1000 chromogenic assay kit (Cambrex Corp., East Rutherford, NJ), and concentrations for the current preparations ranged from 0.02 to 0.07 pg/μg of purified protein. Protein concentrations were determined by the bicinchoninic acid (BCA) assay using BSA as a standard.

Binding and Competition Assays. The binding of trimeric fusion proteins to surface-adsorbed LPS, mannan, or maltosyl-BSA was assessed using 96-well plates and an S-protein-HRP detection system as previously described (*31*, *41*). We obtained a uniform dispersion of LPS (1 mg/mL in binding buffer) by warming the sample to 37 °C and vigorously agitating it for 15 min using a vortex mixer; each subsequent dilution was also performed with vigorous mixing. The wells of 96-well plates (Corning, 3590) were coated with LPS (1−10 μg/mL), or with 50 μg/mL mannan as a control. Washed and coated wells were incubated with blocking/binding buffer containing 1% (w/v) low-endotoxin, low-immunoglobulin fatty acid-free BSA. The proteins were diluted in this buffer in the presence of 5 mM calcium chloride. Coated plates were incubated with fusion protein for 1 h at room temperature, washed, and incubated with S-protein-HRP conjugate (1:2500−5000, Novagen). After the samples had been washed, color was developed using ABTS peroxidase substrate, and the absorbance was measured at 405 nm. Background binding in the absence of fusion protein was subtracted to give total binding. Specific binding was defined as the difference between binding in the absence and presence of 50 mM maltose; for the LPS ligands, nonspecific binding was always <15% of total binding, and usually much lower. In previous experiments, equivalent signals were obtained for various plastic-adsorbed fusion proteins (*31*, *41*), consistent with identical exposure of the N-terminal tags to the S-protein conjugate.

For competition assays, recombinant proteins were preincubated for 30 min in blocking/binding buffer containing 5 mM calcium. The mixture was added to mannan-coated or maltosyl-BSA-coated (*41*) wells in the presence of competitor or EDTA and processed as described for the direct binding assays. Binding and competition data were analyzed using Sigmaplot 9.0 (SPSS Inc., Chicago, IL). Apparent dissociation constants (K_d) and the inhibitor concentration causing 50% inhibition of binding (I_{50}, millimolar or micrograms per milliliter, as indicated) were calculated by nonlinear regression using single-site saturation and competition models, respectively. Although it is not possible to calculate true dissociation constants with this type of assay, the analysis permits quantitative comparison of the binding properties of the homologous NCRD fusion proteins using unmodified ligands. All values are given as the mean ± standard error of the mean (SEM).

Crystallographic Analysis. Crystals were prepared as previously described (*11*). All ligands were dissolved in mother liquor. Crystals were transferred into the resulting solution and soaked for 2−6 h. The final concentrations of ligands were as follows: 330 mM L,D-heptose, 250 mM 2-deoxyheptose, 100 mM 7-carbamoyl derivative, 200 mM D,D-heptose, 100 mM heptose disaccharide, and 100 mM Kdo. After soaking, crystals were briefly dipped in soak solution with 20% MPD (2-methyl-2,4-pentanediol) as cryoprotectant and then flash-frozen in a 100 K stream of nitrogen gas. Data were collected either on a Raxis4 instrument or at beamline X8C at the National Synchrotron Light Source, Brookhaven National Laboratory (Upton, NY).

Data were processed using DENZO and SCALEPACK (*42*). Model building and structure refinement were performed using Coot and CNS, while topology and parameter files for all ligands were obtained using Xplo2d (*12, 43, 44*).

RESULTS

Previous studies have shown specific binding of full-length rat SP-D dodecamers to various forms of R-LPS by ligand blotting of LPS molecules following resolution by SDS−PAGE (*13, 16, 17*). To confirm interactions of the trimeric human NCRDs with LPS, we used a well-characterized SP-D ligand, *E. coli* J-5 LPS, which has a truncated R3 core oligosaccharide with terminal glucose attached to Hep-II (Figure 1A). In preliminary experiments, both human and rat NCRDs showed carbohydrate-sensitive binding to solid-phase J-5 LPS. Binding was largely abrogated by maltose,

Table 1: Apparent Affinities of NCRDs for Solid-Phase R-LPS

	apparent K_d (mean ± SEM × 10^{-8} M)	
trimeric NCRD	*E. coli* J-5 LPS	*E. coli* Rd2-LPS
human wild-type	15.5 ± 3.7 (3)[a]	15.6 ± 1.4 (6)
rat wild-type	2.4 ± 0.6 (3)	2.4 ± 0.9 (3)
human R343K	2.5 ± 0.8 (4)	1.6 ± 1.2 (3)
human R343A	14 (1)	not determined
rat K343R	52 ± 14 (2)	22.8 (2)

[a] Number of independent experiments.

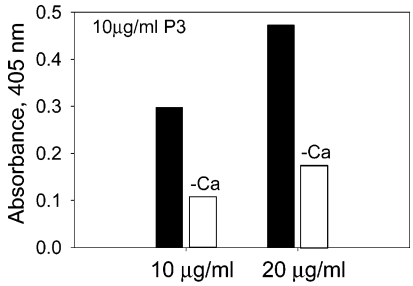

FIGURE 2: Human trimeric NCRDs bind to the purified core OS of J-5 LPS. The dose-dependent binding of the human NCRD fusion protein to nonasaccharide trisphosphate conjugated to BSA was examined in the presence and absence of calcium as described in Experimental Procedures.

the prototypical competitive inhibitor, or EDTA, indicating calcium-dependent binding mediated by the CRD (data not shown). By comparison with the rNCRDs, hNCRDs always exhibited weaker maximum binding (e.g., as shown in Figure 5), and the apparent affinity of the rat protein for J-5 LPS was at least 6-fold greater (Table 1). Similar differences were observed using equivalent coating concentrations of several different available preparations of the J-5 LPS, albeit with some variation in maximum binding among preparations. As previously observed, the human and rat NCRDs showed nearly identical concentration-dependent binding to solid-phase mannan (*41*).

Trimeric NCRDs Bind to the Purified Core Oligosaccharide of J-5 LPS. To confirm interactions with the core OS domain of the LPS, we examined binding to the purified, full-length *E. coli* J-5 LPS nonasaccharide trisphosphate (Figure 1A) coupled to bovine serum albumin (*33*−*35*). The NCRDs exhibited maltose-sensitive binding to the neoglycoproteins (Figure 2). Binding was also significantly inhibited by the absence of calcium (data not shown). Limited amounts of material precluded saturation binding experiments. However, the findings were reproduced in three independent experiments.

Trimeric NCRDs Bind to Solid-Phase Rd-LPS but Not Re-LPS. To further localize binding determinants within the core, we examined interactions with deeper rough LPS mutants. The NCRDs showed concentration-dependent binding to solid-phase Rd2-LPS (Figure 3), which is characterized by further truncation of the core (Figure 1B). As for J-5 LPS, binding was both calcium-dependent and saccharide-sensitive (data not shown). Maximum binding of the human protein was weaker than that observed for the rat, but the magnitude of this difference was smaller at all examined coating concentrations. Nevertheless, the apparent affinity of the hNCRD for Rd-LPS was several-fold lower than that observed for the rNCRD and comparable to that observed for J-5 LPS (Table 1). Consistent with earlier work using

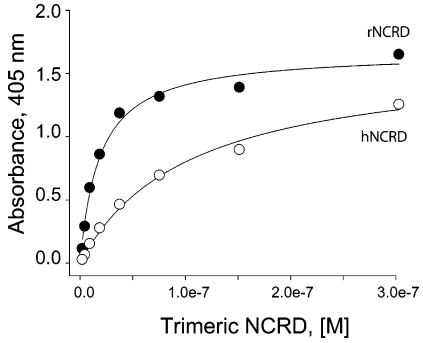

FIGURE 3: Trimeric NCRDs bind to solid-phase Rd2-LPS. The dose-dependent, specific binding of rat and human NCRD fusion proteins to *E. coli* Rd2-LPS (10 μg/mL) was examined as it was for the J5 LPS.

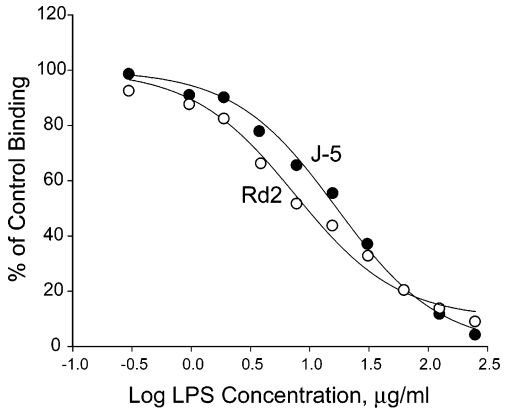

FIGURE 4: Trimeric NCRDs bind to R-LPS micelles and aggregates. The binding of the wild-type human NCRD fusion protein (20 μg/mL) to J-5 and Rd2-LPS was examined at room temperature in competition assays using mannan as the solid-phase ligand. LPS concentrations spanned the very approximate, nominal critical micelle concentration (15 μg/mL). R-LPS caused a dose-dependent inhibition, and complete inhibition of binding was achieved at concentrations greater than approximately 100 μg/mL. Although inhibitory activity varied with the specific preparation of LPS, Rd2-LPS was at least as potent as J-5 LPS.

rat SP-D (*13*), neither protein showed calcium-dependent or sugar-sensitive binding to immobilized Re-LPS from *S. enterica* sv. Minnesota, a deep rough mutant that terminates with the α2→4-linked Kdo disaccharide and lacks heptose or glucose (data not shown).

Trimeric NCRDs Bind to R-LPS Micelles and Aggregates. To further confirm these interactions in the solution phase, we examined the ability of suspensions of LPS to compete for the binding of the NCRDs to solid-phase mannan. Under the conditions of physiological ionic strength, pH, and calcium concentration, the dilutions of LPS, which span the nominal critical micelle concentration (CMC), are expected to contain varying proportions of LPS monomers and micellar and/or complex layered arrangements of LPS molecules. As illustrated in Figure 4, suspensions of Rd2 and J-5 LPS exhibited dose-dependent inhibition of human NCRD binding to mannan. The inhibitory activity of Rd2 was slightly greater [16 ± 4 and 30 ± 17 μg/mL (n = 3), respectively]. Similar dose-dependent inhibition was observed for the rat protein, with average I_{50} values of approximately 20 μg/mL for both forms of LPS (data not shown).

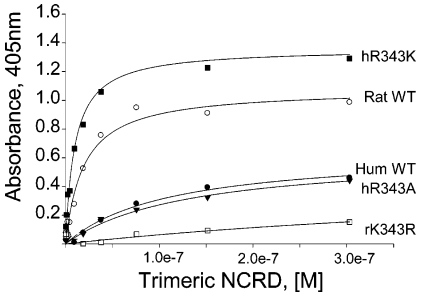

FIGURE 5: Residue 343 contributes to R-LPS recognition. The dose-dependent, specific binding of rat and human NCRD fusion proteins to *E. coli* J-5 LPS (1 μg/mL) was examined, as described in Experimental Procedures. The substitution of lysine at position 343 in the human NCRD (hR343K) greatly enhances binding relative to that of the wild-type (WT) human form. The substitution of arginine at position 343 in rat SP-D (rK343R) greatly reduces the level of binding compared to that of the wild-type rat form. The findings localize LPS binding to the vicinity of the carbohydrate binding site of the SP-D CRD.

Table 2: Apparent Affinities for Maltose

trimeric NCRD	I_{50} (mM; mean ± SEM)
human wild-type (*41*)	2.7 ± 0.4 (11)
rat wild-type (*41*)	0.55 ± 0.08 (10)
human R343K[a]	0.35 ± 0.04[b] (4)
human R343A	1.6 ± 0.18[b] (3)
rat K343R	1.4 ± 0.26[c] (5)

[a] Using maltosyl-BSA as the solid-phase ligand. [b] Significantly different from that of the wild-type human form ($p < 0.05$). [c] Significantly different from that of the wild-type rat form ($p < 0.05$).

The Nonconserved Residue at Position 343 Contributes to R-LPS Recognition. The solid-phase binding data indicate differences in LPS recognition by rat and human lectin domains. Human SP-D contains Arg343, while this position is occupied by lysine in all other known SP-Ds, including rat and mouse forms. Given the known effects of residue 343 on binding to other glycoconjugates and PI, we explored the hypothesis that nonconserved residues adjacent to calcium at the carbohydrate binding site contribute to R-LPS recognition.

Although lysine is nominally a conservative substitution, we initially examined a human mutant with the substitution of lysine for arginine 343 (hR343K). As illustrated in Figure 5 and summarized in Table 1, hR343K showed stronger binding to J-5 and Rd2-LPS. The apparent affinity was also increased, compared to that of the human form, and not significantly different from that of the wild-type rat protein (Table 1). By contrast, this mutant showed greatly weakened binding to mannan (*12*). The apparent affinity for maltose was also increased, to levels comparable to that of the wild-type rat form (Table 2). However, there was only a small increase in affinity for D-mannose, and no significant change in affinity for *N*-acetylmannosamine (data not shown), a preferred ligand for the human protein (*41*).

We also examined the LPS binding activity of a reciprocal rat mutant with a substitution of arginine for lysine at position 343 (rK343R). Rat K343R binds efficiently to mannan, which is comparable to that of the wild-type rat and human NCRDs (*12*). Nevertheless, the level of binding of rat K343R

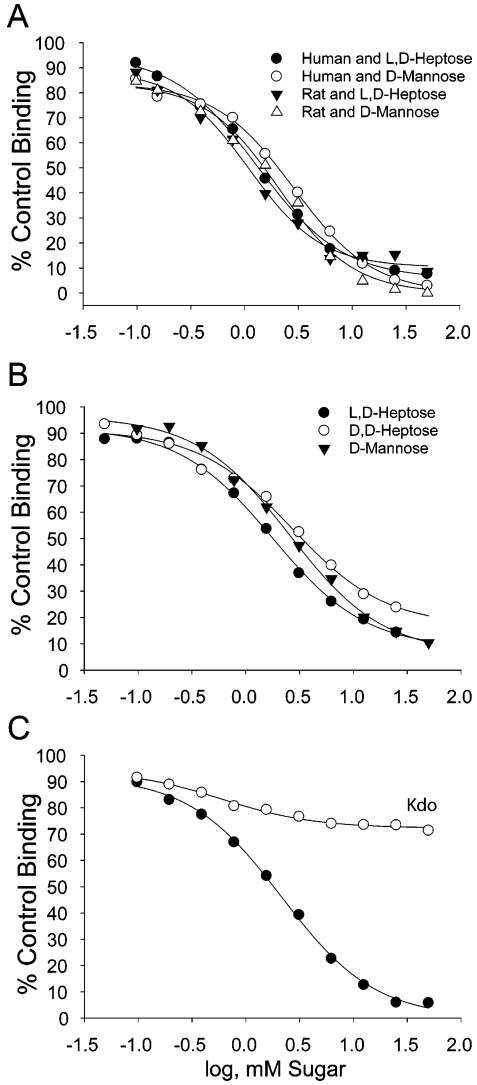

FIGURE 6: Competition with heptoses and Kdo. The binding of heptoses and Kdo to wild-type NCRD fusion proteins (5 μg/mL) was examined in competition assays using mannan as the solid-phase ligand. (A) Binding of rat NCRD to L,D-heptose (▼), human NCRDs to L,D-heptose (●), rat NCRDs to D-mannose (△), and human NCRDs to D-mannose (○). (B) Binding of human NCRDs to L,D-heptose (●), D,D-heptose (○), and D-mannose (▼). (C) Binding of human NCRDs to Kdo (○) and maltose (●). I_{50} values are summarized in Table 3.

to J-5 LPS was greatly decreased as compared to that of wild-type rat NCRD, and the apparent affinity was decreased in two independent determinations (Figure 5 and Table 1). The level of binding to Rd2-LPS was also decreased and more comparable to that of the wild-type human form (Table 1). Thus, lysine 343, whether occurring in the context of the mutant human or wild-type rat protein, enhances interactions with J-5 and Rd2-LPS.

To further confirm the dependence on the amino acid side chain, we examined a mutant with alanine at position 343 in the human protein (hR343A). Previous studies have shown that the affinity of hR343A for mannan is comparable to that of the wild type (*12*). The level of binding of hR343A to J-5 LPS was only slightly increased compared to that of the human NCRD and substantially lower than that of hR343K or wild-type rat NCRDs (Figure 5). The apparent affinity was not different from that of the human protein in

Table 3: Apparent Affinities of hNCRD for Heptoses

competing ligand	I_{50} (mM; mean ± SEM)
D-mannose	2.7 ± 0.13 (3)
D-maltose	2.3 ± 0.18 (3)
L,D-heptose	1.5 ± 0.13 (3)
D,D-heptose	2.7 (1)
2-deoxyheptose	not determined
7-carbamoyl-L,D-heptose	1.7 (1)

the single-saturation binding experiment that used the same preparation of LPS (Table 1). There was also no significant effect of the interspecies substitution of asparagine for aspartate at position 325 (data not shown), a substitution previously observed to enhance mannan binding (*41*).

Human NCRDs Bind to Heptose. L-*glycero*-D-*manno*-Heptose is the most common heptose found in the core regions of Gram-negative bacteria and is present in all forms of LPS known to react with SP-D. As shown in Figure 6A and Table 3, highly purified L,D-heptose was an efficient competitor of SP-D binding to mannan, and the I_{50} values of rat and human NCRDs were similar. Although the number of determinations is small, the apparent affinity appears to be increased relative to that of D-mannose. Similar inhibitory activity was obtained for D,D-heptose (Figure 6B), and a 7-*O*-carbamoyl derivative of L,D-heptose (Table 3). In one experiment, a 7-phosphate derivative of D,D-heptose showed no inhibitory activity (data not shown). Purified Kdo was also an ineffective competitor (Figure 6C).

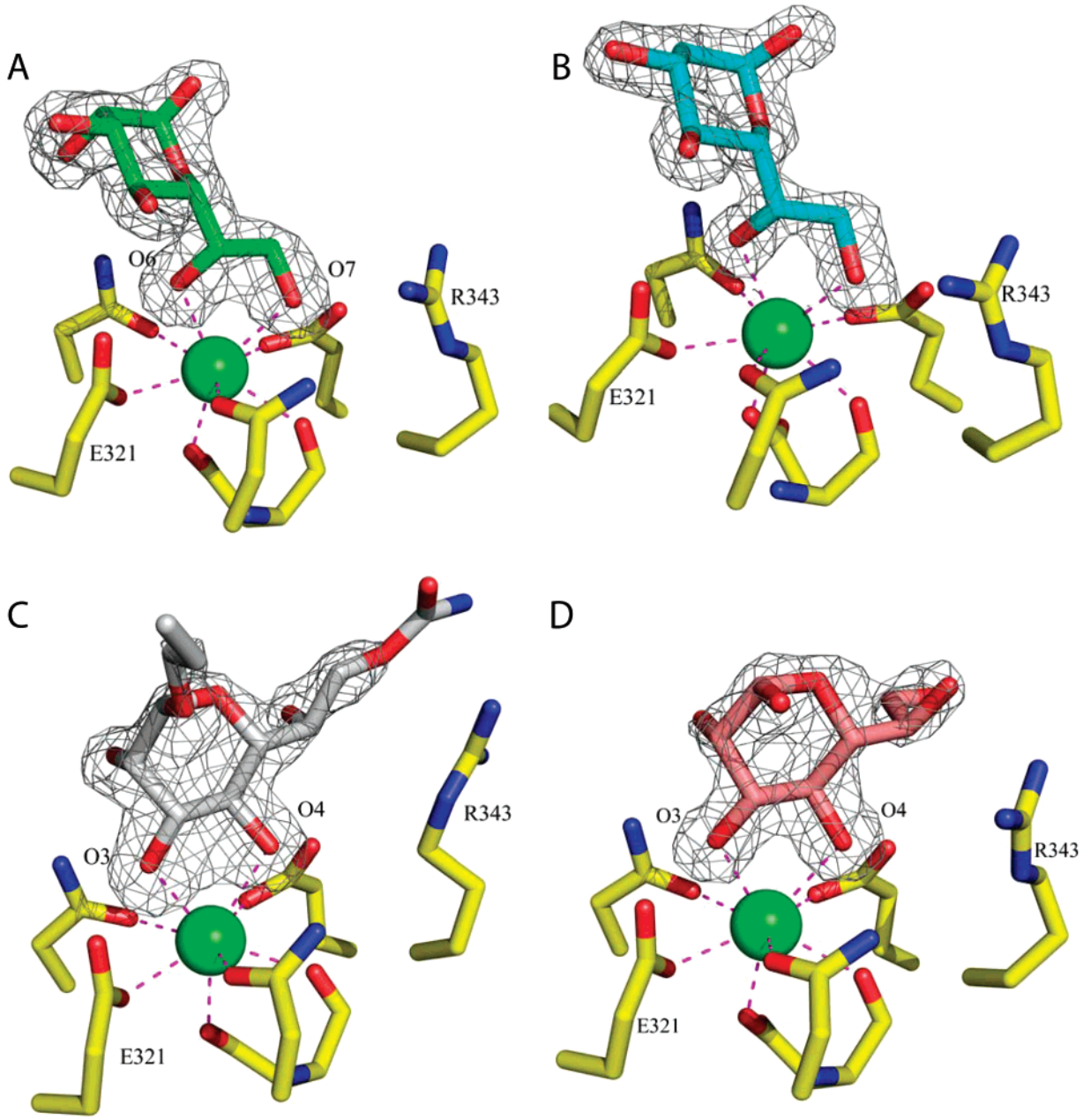

FIGURE 7: Crystallographic complexes of the wild-type human NCRD with L,D-heptoses and D,D-heptose. (A) L,D-Heptose (red and green sticks) binds to Ca1 (green) by the 6- and 7-OH groups of its side chain. (B) 2-Deoxyheptose (aqua and red sticks) also interacts with Ca1 via the side chain. (C) The 7-carbamoyl derivative of L,D-heptose binds to Ca1 via the equatorial 3- and 4-OH groups of the pyranose ring, with the carbamoyl group pointing toward, but not H-bonding to R343. (D) D,D-Heptose (red and pink sticks) also interacts with Ca1 via the sugar ring. Electron density maps are $F_o - F_c$ simulated annealing omit maps of the ligands, contoured at 3σ. H-Bonding patterns are given in Table 4. Data collection and refinement statistics are listed in Table 5.[2]

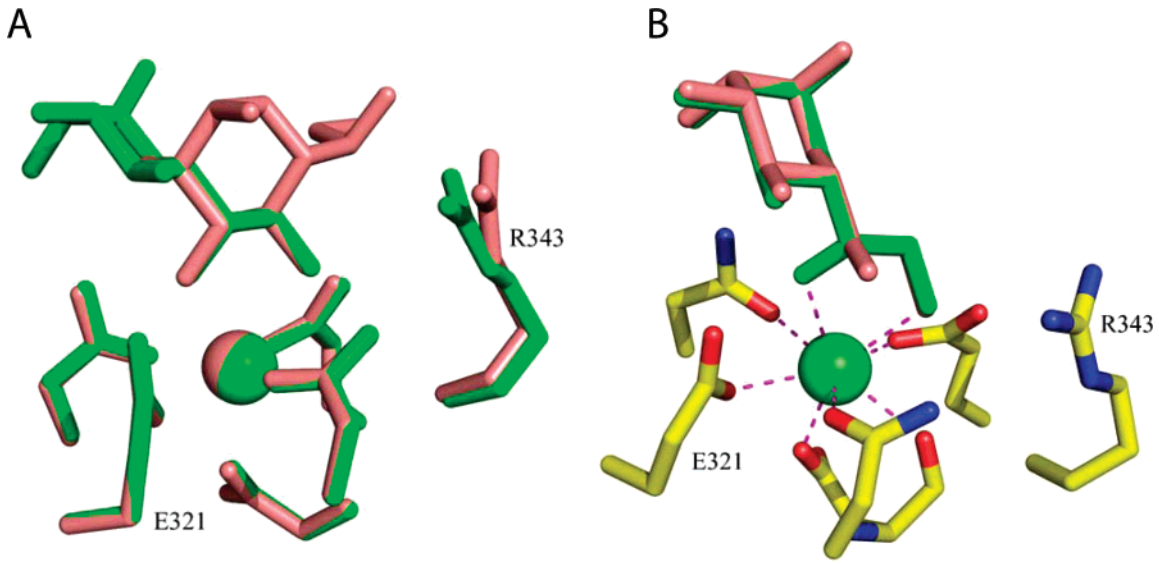

FIGURE 8: Superimpositions of L,D- and D,D-heptose. (A) D,D-Heptose (pink sticks) and L,D-heptose (green sticks) crystal complexes illustrated in panels A and D of Figure 7 were aligned. The side chain OH groups of L,D-heptose show the same spatial distribution as the vicinal OH groups of the pyranose ring of D,D-heptose. (B) D,D-Heptose (pink sticks) was reoriented and superimposed on the L,D-heptose crystal structure (green sticks). The spatial distribution of the 6- and 7-OH groups of the side chain of D,D-heptose does not allow coordination with Ca1.

Crystallographic Analysis Demonstrates Binding via the L-Glyceryl Side Chain of L,D-Heptose.[2] To define how SP-D interacts with heptose, crystal structures of human NCRD in complex with selected heptose forms were determined (Figure 7). Electron density corresponding to bound L,D-heptose was well-represented in all three subunits of the NCRD (Figure 7A). However, the mode of binding differed from that of previously characterized saccharide−NCRD complexes in that the side chain coordinated with Ca1 via the 6-OH and 7-OH groups. In all previous structures of SP-D bound with sugars or inositols, binding involved vicinal OH groups of the sugar ring (*11*, *12*). The positions of the glyceryl OH groups of L,D-heptose in the complex were almost superimposed on those of the equatorial 3- and 4-OH groups in our previous ligand structures. The ring orientation in the bound L,D-heptose was stabilized in part by a H-bond between the 2-OH group and ND2 of N323. To assess the significance of this interaction, we also determined the structure of the 2-deoxy derivative of L,D-heptose but found that the binding orientation, via 6- and 7-OH groups, was unchanged (Figure 7B). A slight tilting of the ring enabled a new H-bond to form between O5 and ND2 of N323. Substitution at the C7-OH group of L,D-heptose, as in 7-*O*-carbamoyl-L,D-heptose, was found to force the ligand to bind by the ring, in an orientation similar to that of the D,D-heptose (Figure 7C). However, the carbamoyl group and the O1-linked allyl substituent of this ligand were disordered.

Because D,D-heptose can occasionally be found in the LPS inner core, and given the importance of the L-glyceryl group for binding to L,D-heptose, we also examined complexes with this sugar (Figure 7D). Electron density corresponding to bound D,D-heptose was present in all three subunits of the NCRD complex, although the density was weak in subunit A. D,D-Heptose bound to Ca1 by the sugar ring, using the equatorial 3-OH and 4-OH groups, identical to previous monosaccharide structures and the 7-carbamoyl derivative. As shown in Figure 8A, the vicinal hydroxyl groups of D,D-heptose could be superimposed on the side chain hydroxyl groups of L,D-heptose. On the other hand, superimposition of a reoriented D,D-heptose on the L,D-heptose structure (Figure 8B) demonstrated that the 6- and 7-OH groups of the side chain of D,D-heptose cannot be similarly oriented to coordinate with Ca1.

The sugar ring and all ring hydroxyl groups of D,D-heptose were well-represented by electron density in the B and C subunits; however, the density of the side chains beyond C6 was weak. Binding by the ring orients the L-glyceryl moiety toward R343. Although there was some displacement of the R343 side chain away from the ligand (Figure 8A), there was no evidence of hydrogen bonding. This appears to leave the side chain free to rotate around the C6−C7 bond, giving little electron density beyond C6.

Kdo, an octulosonic sugar acid with a side chain similar to the side chain of D,D-heptose, is a ubiquitous component of the LPS inner core. Although Kdo was an ineffective competitor of binding of SP-D to mannan and lacks vicinal OH groups suitable for coordination to calcium, crystals soaked with Kdo showed some electron density in the binding sites of all three subunits (data not shown). Most of the density for this ligand was poorly defined but could be modeled as an unconventional complex with one of the coordinating oxygen atoms contributed by the 2-OH group of the ring and the second by the 1-carboxylate group.

Crystallographic Complex with a Diheptose. To further assess interactions of SP-D with the LPS inner core, the structure of the NCRD complexed with α1→3-linked heptose disaccharide was also determined. This corresponds to the Hep-I and Hep-II present in many LPS core structures. Electron density corresponding to both Hep-I and Hep-II was

[2] Atomic coordinates for the crystal structures of this protein have been submitted to the Research Collaboratory for Structural Bioinformatics Protein Data Bank as entries 2RIA, 2RIB, 2RIC, 2RID, and 2RIE.

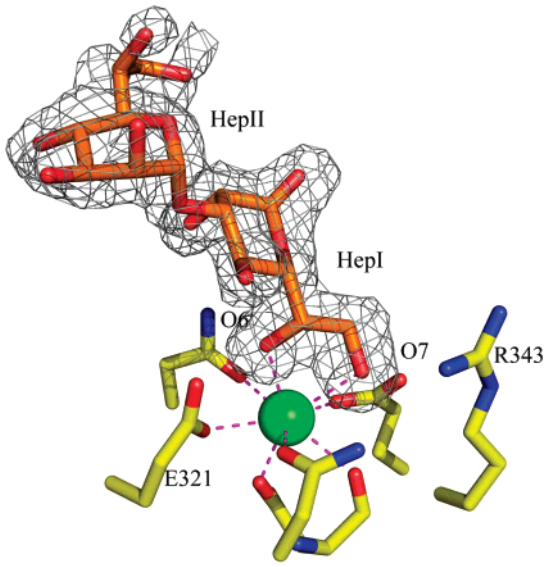

FIGURE 9: Crystallographic complex with a heptose disaccharide. We also examined complexes with heptose disaccharide, i.e., L-*glycero*-α-D-*manno*-heptopyranosyl(1→3)-L-*glycero*-α-D-*manno*-heptopyranose. This disaccharide corresponds to Hep-I and Hep-II of the inner core. Notably, binding was exclusively mediated by the side chain of Hep-I. Heptose disaccharide is shown in red and orange sticks. Electron density maps are $F_o - F_c$ simulated annealing omit maps of the ligands, contoured at 3σ.

well-represented in subunit B, with Hep-I binding to Ca1 by the 6-OH and 7-OH groups (Figure 9). Other protein molecules packed in the crystal impose constraints on binding of the heptose disaccharide in subunits A and C. In subunit C, only Hep-I is well-defined, bound as in subunit B, but the electron density for Hep-II is broken. In subunit A, where there is the closest approach of an NCRD packing mate, there was little evidence of the ligand.

DISCUSSION

These studies demonstrate specific interactions of the carbohydrate binding regions of the SP-D lectin domain with the core oligosaccharide of enteric LPS. In aggregate, the data suggest a dominant role of carbohydrate interactions in recognition of this important bacterial glycoconjugate and strongly implicate inner core heptose as the primary site of the carbohydrate interaction, at least for Rd-LPS.

Crystallographic analysis revealed a novel, selective, and stereospecific mode of interaction between the C6- and C7-OH groups of L,D-heptose and Ca1 at the carbohydrate binding site. More importantly, the side chain of Hep-I of the heptose disaccharide exhibited the same mode of interaction. This binding orientation leaves hydroxyl groups available for participation in glycosidic linkages with Kdo, Hex-I, and Hep-III, when placed within the context of an enteric LPS. These observations have diverse and important implications for LPS recognition.

First, interactions with the heptose side chain provide a potential mechanism of inner core recognition that does not require exposed 3- and 4-OH groups on the sugar ring. Because the inner core is highly conserved, interactions with nonterminal L,D-heptose residues provide a reasonable explanation for interactions with diverse types of LPS, even in the absence of exposed vicinal 3- and 4-OH groups on Hep-I, Hep-II, or other sugars.

Table 4: Hydrogen Bonds between SP-D and Ligands

		distance (Å)		
atom 1	atom 2	chain A	chain B	chain C
		l,d-Heptose		
6-OH	Glu321 OE2	2.50	2.56	2.52
	Asn323 ND2	3.19	3.00	3.22
	Asn341 OD1	2.98	3.30	3.27
7-OH	Asn341 ND2	3.16	3.02	3.02
	Glu329 OE2	2.69	2.68	2.63
	Asp342 O	N/A[a]	3.32	3.30
2-OH	Asn323 ND2	3.27	3.25	3.18
		2-Deoxyheptose		
6-OH	Glu321 OE2	2.54	2.61	2.57
	Asn323 ND2	3.01	2.91	3.03
	Asn341 OD1	3.09	3.34	3.34
7-OH	Asn341 ND2	3.10	3.01	3.01
	Glu329 OE2	2.69	2.62	2.60
	Asp342 O	3.34	3.21	3.17
5-OH	Asn323 ND2	3.27	3.26	3.03
		d,d-Heptose		
3-OH	Glu321 OE2	2.66	2.47	2.62
	Asn323 ND2	N/A[a]	3.05	N/A[a]
	Asn341 OD1	2.88	3.19	2.89
4-OH	Asn341 ND2	3.18	3.07	3.19
	Glu329 OE2	2.62	2.56	2.59
	Asp342 O	3.33	N/A[a]	N/A[a]
		Diheptose		
6-OH	Glu321 OE2	2.60	2.61	2.65
	Asn323 ND2	N/A[a]	3.06	3.10
	Asn341 OD1	3.00	3.28	3.31
7-OH	Asn341 ND2	N/A[a]	3.07	2.97
	Glu329 OE2	2.64	2.62	2.61
	Asp342 O	N/A[a]	N/A[a]	3.25
2-OH/5-O	Asn323 ND2	3.35 (5-O)	3.22 (2-OH)	3.24 (2-OH)
		7-Carbamoyl-Heptose		
3-OH	Glu321 OE2	2.56	2.55	2.49
	Asn323 ND2	3.03	2.99	2.99
	Asn341 OD1	N/A[a]	3.22	3.34
4-OH	Asn341 ND2	3.20	3.13	3.12
	Glu329 OE2	2.62	2.54	2.63
	Asp342 O	N/A[a]	3.34	N/A[a]
6-OH	Asp325 OD2	N/A[a]	2.71	2.94
2-OH	Asp325 OD2	N/A[a]	3.01	2.73
2-OH	Asn323 ND2	N/A[a]	N/A[a]	3.22

[a] Not available.

Second, some respiratory pathogens show characteristic modifications of specific heptoses that can now be predicted to alter recognition by SP-D. For example, the LPS of several *P. aeruginosa* strains is characterized by a 7-*O*-carbamoyl substitution of L,D-Hep-III (*45*−*48*), which precludes interactions with the side chain. Notably, *P. aeruginosa* LPS also shows a higher degree of phosphorylation of the heptose residues than *E. coli* LPS. In addition, *K. pneumoniae* LPS characteristically shows a negatively charged substituent (β-GalUA) at position 7 of Hep-III, but no phosphate on any of the heptose residues. D,D-Heptose is restricted to a smaller subset of Gram-negative bacteria, and our findings suggest that it could only contribute to SP-D binding if exposed as a terminal sugar.

Third, many Gram-negative bacteria show nonstoichiometric modifications of the conserved inner core oligosaccharide, leading to structural variations and microheterogeneity (*3*). Although still poorly understood, these enzymatically catalyzed modifications are subject to regulation by environmental or growth conditions, and some are known to alter membrane permeability. Potential nonstoichiometric heptose

Table 5: Statistics from Data Collection and Refinement

	L,D-heptose	2-deoxyheptose	diheptose	D,D-heptose	carbamoyl derivative
			Diffraction Data		
wavelength (Å)	1.5418	1.1000	1.5418	1.5418	1.5418
resolution (Å)	1.80	1.60	1.80	1.80	1.80
space group	$P2_1$	$P2_1$	$P2_1$	$P2_1$	$P2_1$
unit cell dimensions					
a (Å)	55.200	55.285	55.404	55.414	55.603
b (Å)	107.441	108.180	107.531	108.606	108.615
c (Å)	55.506	55.543	55.698	55.548	55.628
β (deg)	91.513	90.992	90.280	91.028	90.907
no. of reflections	59219	83562	57647	58216	59548
completeness[a] (%)	98.6 (85.3)	97.3 (87.8)	95.3 (68.3)	95.6 (92.6)	97.5 (87.0)
redundancy[a]	3.0 (2.5)	5.2 (2.3)	3.4 (2.3)	2.7 (2.4)	2.7 (2.0)
R_{merge}[a,b] (%)	4.8 (24.3)	3.2 (17.5)	4.9 (37.2)	7.4 (30.3)	6.6 (35.6)
			Refinement		
resolution range (Å)	50−1.8	50−1.6	50−1.8	50−1.8	50−1.8
R_{cryst}[c]	0.1864	0.1986	0.2050	0.2089	0.2051
R_{free}[d]	0.2040	0.2120	0.2299	0.2369	0.2320
no. of protein atoms	3459	3347	3540	3345	3421
no. of ions	9	9	9	9	9
no. of water molecules	460	554	427	378	392
rmsd[e] for angles (deg)	1.1374	1.1369	1.1102	1.1447	1.1427
rmsd[e] for bonds (Å)	0.0051	0.0048	0.0054	0.0053	0.0055
mean $\langle B \rangle$ for protein (Å^2)[f]	26.7	21.1	32.9	26.0	27.8
mean $\langle B \rangle$ for ligand (Å^2)[f]	28.2	23.9	42.4	35.5	39.7
Ramachandran plot (%)[g]					
most favored	93.6	93.3	94.5	91.7	92.2
additional allowed	6.4	6.7	5.5	8.3	7.8

[a] Completeness, redundancy, and R_{merge} reported for all reflections and for the highest-resolution shell (values in parentheses). [b] $R_{merge} = \sum|I_i - \langle I \rangle|/\sum I_i$, where I_i is the intensity of an individual reflection and $\langle I \rangle$ is the mean intensity of that reflection. [c] $R_{cryst} = \sum||F_p| - |F_{calc}||/\sum|F_p|$, where $|F_{calc}|$ and $|F_p|$ are the calculated and observed structure factors, respectively. [d] R_{free} defined as in Brünger. [e] Root-mean-square deviation. [f] Calculated using Moleman. [g] Calculated using Procheck.

modifications include phosphorylation or substitutions with *PP*Etn, *N*-acetylglucosamine, or glucosamine. Such effects could prove to be significant, if not critical, determinants of SP-D recognition for specific organisms. For example, phosphorylation at position 7 of D,D-heptose rendered the sugar ineffective as a competitor. Thus, nonstoichiometric or constitutive modifications of heptose introduce an element of complexity in LPS recognition that has previously not been considered in the context of innate immune recognition by any LPS binding protein.

Mechanism of Heptose Recognition. The molecular basis for the stereospecific interaction of the human NCRD with the side chain of L,D-heptose is evident from the crystallographic analyses. The OH groups at C6 and C7 can assume a conformation similar to that of the equatorially oriented OH groups at C3 and C4 and participate in direct interactions with Ca1 at the carbohydrate binding site. This interaction is stabilized by H-bonds with coordinating amino acids in a manner virtually identical to that of mannose or other simple sugars (Table 4) (*9*−*12*). This configuration is not possible with the side chain hydroxyl groups in D,D-heptose (Figure 8B). It is less clear why the human NCRD so preferentially selects the side chain over the vicinal OH groups of the ring. The apparent affinity for L,D-heptose was only slightly higher than that for D-mannose (Table 3). We saw no evidence of the latter mode of interaction with the ring OH groups in any of the three subunits with either L,D-heptose or 2-deoxy-L,D-heptose. When the 7-OH group of L,D-heptose was blocked with the carbamoyl moiety, the binding affinity was comparable to that of L,D-heptose; however, binding was exclusively mediated by the 3- and 4-OH groups of the pyranose ring.

Unconventional Interactions of Kdo with Ca1. Kdo is a key structural component of the inner core, providing the linkage between lipid A and the core oligosaccharide. Thus, low affinity for this sugar is consistent with poor binding to Re-LPS and further supports the importance of heptose recognition for observed interactions with Rd-LPS. Although some weak occupancy of the carbohydrate binding site was observed, these interactions were apparently restricted to the 2-OH group and the 1-carboxyl group. Because the 2-OH group of Kdo normally participates in a glycosidic linkage, this weak interaction is unlikely to be relevant to observed interactions with LPS.

Species Differences in LPS Recognition by NCRDs. In the original studies of SP-D−LPS interactions, rat and human SP-D were found to interact with LPS and various Gram-negative bacteria (*13*). Ligand blots of various truncated forms of LPS showed preferential interactions of SP-D dodecamers with rough forms of LPS that were isolated from rough mutants of *E. coli* or *S. enterica* sv. Minnesota (*13*). However, the human and rat proteins were not directly compared, and all experiments that aimed to examine the interactions of SP-D with various forms of LPS used iodinated rat SP-D. In the studies presented here, we observed significant differences in LPS recognition by the lectin domains of rat and human SP-D. Given the diversity of forms of LPS known to be recognized by SP-D, and the wide range of concentrations potentially encountered in vivo, it is important to avoid the inference that human SP-D is intrinsically less active than rat SP-D with respect to interactions with LPS or Gram-negative bacteria. Although the affinity of the human protein was lower for solid-phase R-LPS, this was influenced by ligand density (data not

shown), and there were less marked differences in maximum binding for Rd2-LPS. Notably, the rat and human proteins were similarly inhibited by LPS micelles and aggregates.

Contributions of Arg/Lys343 to LPS Recognition. Interactions of the CRD with LPS were substantially influenced by the amino acid side chain at position 343, definitively demonstrating interactions between LPS and the carbohydrate binding region of the CRD. Although residue 343 is not a calcium ligand, it resides on the C-terminal ridge of the shallow carbohydrate binding groove. Allen and co-workers showed that the substitution of valine for Arg343 increases the affinity of human SP-D for α-methyl glucoside by approximately 3-fold (*49*). The substitution of lysine for Arg343 in the hNCRD even more substantially increased the apparent affinity for maltose, while the reciprocal substitution of arginine for lysine in the rat NCRD decreased the affinity. We do not currently have sufficient amounts of the purified heptoses to permit systematic comparisons of I_{50} values for the NCRD mutants. However, changes in the apparent affinity for the prototypical competitor, maltose, an α-1,4-linked glucose disaccharide, paralleled observed differences in binding to R-LPS. Given that glucosamine is believed to be a poor ligand, it is possible that preferential interactions of the rat protein and hR343K with J-5 LPS reflect enhanced interactions with the terminal glucose residue of *E. coli* J-5 LPS (*2*). However, preferences for terminal sugars cannot readily account for the greater affinity of the rNCRD and R343K for Rd2-LPS. Rat and human SP-D showed nearly identical affinities for L,D-heptose. It is possible that binding is differentially affected by nonstoichiometric modifications of Hep-I, or by the contiguous lipid A domain. Studies using Rd2-LPS of more defined structure and/or truncated core oligosaccharides will be needed.

Elucidation of the specific contributions of the Lys343 side chain to R-LPS binding will require crystallographic analysis of rat SP-D and/or human R343K. However, on the basis of preliminary modeling, we speculate that Lys343 participates in additional stabilizing interactions with nonterminal core sugars and/or their associated modifications. Notably, SP-D possesses an extended ligand binding site that involves residues even more remote from Ca1 (*11*); a variety of unpublished observations suggest differential utilization of the extended site by different complex ligands.

Ligand preferences can also be influenced by the higher-order oligomerization of trimeric subunits (*41*, *50*). Recent studies demonstrated that full-length, natural human trimers bind more efficiently to certain forms of LPS than dodecamers (*50*). Accordingly, interactions with full-length proteins are being reexamined. However, such experiments are substantially more complex given the incomplete cross reactivity of the antibodies used in assays, potential effects of antibody binding on lectin function, and/or the effects of modifications introduced by labeling procedures.

In summary, we present evidence that binding of SP-D to R-LPS is mediated by interactions between the carbohydrate binding site of the CRD and the inner core OS of the lipopolysaccharide. Interactions with L,D-heptose involve the carbohydrate side chain, thereby permitting interactions with core heptoses participating in an α1→3 glycosidic linkage. Importantly, these interactions can be altered by nonstoichiometric modifications at the 7-OH group. The biological significance of observed species differences remains to be determined but suggests evolutionary divergence in the recognition of specific core oligosaccharides by the human protein.

ACKNOWLEDGMENT

We thank Alla Zamaytina and Hassan Amer for providing the heptose saccharides and Edit Balla for the synthesis of 2-deoxyheptose. We thank Bruce Linders and Veronika Susott for technical assistance and Janet North for administrative support.

REFERENCES

1. Raetz, C. R., and Whitfield, C. (2002) Lipopolysaccharide endotoxins, *Annu. Rev. Biochem. 71*, 635−700.
2. Holst, O., and Brade, H. (1992) in *Bacterial endotoxic lipopolysaccharides* (Morrisson, D. C., and Ryan, J. L., Eds.) pp 135−170, CRC Press, Boca Raton, FL.
3. Frirdich, E., and Whitfield, C. (2005) Lipopolysaccharide inner core oligosaccharide structure and outer membrane stability in human pathogens belonging to the Enterobacteriaceae, *J. Endotoxin Res. 11*, 133−144.
4. Crouch, E. C. (2006) in *Encyclopedia of Respiratory Medicine* (Laurent, G., and Shapiro, S., Eds.) pp 152−158, Elsevier Limited, Oxford, U.K.
5. Kishore, U., Greenhough, T. J., Waters, P., Shrive, A. K., Ghai, R., Kamran, M. F., Bernal, A. L., Reid, K. B., Madan, T., and Chakraborty, T. (2006) Surfactant proteins SP-A and SP-D: Structure, function and receptors, *Mol. Immunol. 43*, 1293−1315.
6. Wright, J. R. (2005) Immunoregulatory functions of surfactant proteins, *Nat. Rev. Immunol. 5*, 58−68.
7. Whitsett, J. A. (2005) Surfactant proteins in innate host defense of the lung, *Biol. Neonate 88*, 175−180.
8. Holmskov, U., Thiel, S., and Jensenius, J. C. (2003) Collections and ficolins: Humoral lectins of the innate immune defense, *Annu. Rev. Immunol. 21*, 547−578.
9. Shrive, A. K., Tharia, H. A., Strong, P., Kishore, U., Burns, I., Rizkallah, P. J., Reid, K. B., and Greenhough, T. J. (2003) High-resolution structural insights into ligand binding and immune cell recognition by human lung surfactant protein D, *J. Mol. Biol. 331*, 509−523.
10. Hakansson, K., Lim, N. K., Hoppe, H. J., and Reid, K. B. (1999) Crystal structure of the trimeric α-helical coiled-coil and the three lectin domains of human lung surfactant protein D, *Struct. Folding Des. 7*, 255−264.
11. Crouch, E., McDonald, B., Smith, K., Cafarella, T., Seaton, B., and Head, J. (2006) Contributions of phenylalanine 335 to ligand recognition by human surfactant protein D: Ring interactions with SP-D ligands, *J. Biol. Chem. 281*, 18008−18014.
12. Crouch, E., McDonald, B., Smith, K., Roberts, M., Mealy, T., Seaton, B., and Head, J. (2007) Critical Role of Arg/Lys343 in the Species-Dependent Recognition of Phosphatidylinositol by Pulmonary Surfactant Protein D, *Biochemistry 46*, 5160−5169.
13. Kuan, S. F., Rust, K., and Crouch, E. (1992) Interactions of surfactant protein D with bacterial lipopolysaccharides. Surfactant protein D is an *Escherichia coli*-binding protein in bronchoalveolar lavage, *J. Clin. Invest. 90*, 97−106.
14. Lim, B. L., Wang, J. Y., Holmskov, U., Hoppe, H. J., and Reid, K. B. (1994) Expression of the carbohydrate recognition domain of lung surfactant protein D and demonstration of its binding to lipopolysaccharides of Gram-negative bacteria, *Biochem. Biophys. Res. Commun. 202*, 1674−1680.
15. Sahly, H., Ofek, I., Podschun, R., Brade, H., He, Y., Ullmann, U., and Crouch, E. (2002) Surfactant protein D binds selectively to *Klebsiella pneumoniae* lipopolysaccharides containing mannose-rich O-antigens, *J. Immunol. 169*, 3267−3274.
16. Pikaar, J. C., van Golde, L. M. G., van Strijp, J. A. G., and Van Iwaarden, J. F. (1995) Opsonic activities of surfactant proteins A and D in phagocytosis of Gram-negative bacteria by alveolar macrophages, *J. Infect. Dis. 172*, 481−489.
17. Ofek, I., Mesika, A., Kalina, M., Keisari, Y., Podschun, R., Sahly, H., Chang, D., McGregor, D., and Crouch, E. (2001) Surfactant protein D enhances phagocytosis and killing of unencapsulated phase variants of *Klebsiella pneumoniae*, *Infect. Immun. 69*, 24−33.

18. Bufler, P., Schmidt, B., Schikor, D., Crouch, E. C., Bauernfeind, A., and Griese, M. (2002) Surfactant protein A and D differently regulate the immune response to non-mucoid *P. aeruginosa* and its lipopolysaccharide, *Am. J. Respir. Cell Mol. Biol. 28*, 249−256.
19. Restrepo, C., Dong, Q., Savov, J., Mariencheck, W., and Wright, J. R. (1998) Surfactant protein D stimulates phagocytosis of *Pseudomonas aeruginosa* by alveolar macrophages, *Am. J. Respir. Cell Mol. Biol. 21*, 576−585.
20. Giannoni, E., Sawa, T., Allen, L., Wiener-Kronish, J., and Hawgood, S. (2006) Surfactant proteins A and D enhance pulmonary clearance of *Pseudomonas aeruginosa*, *Am. J. Respir. Cell Mol. Biol. 34*, 704−710.
21. Schaeffer, L. M., McCormack, F. X., Wu, H., and Weiss, A. A. (2004) Interactions of pulmonary collectins with *Bordetella bronchiseptica* and *Bordetella pertussis* lipopolysaccharide elucidate the structural basis of their antimicrobial activities, *Infect. Immun. 72*, 7124−7130.
22. LeVine, A. M., Whitsett, J. A., Gwozdz, J. A., Richardson, T. R., Fisher, J. H., Burhans, M. S., and Korfhagen, T. R. (2000) Distinct effects of surfactant protein A or D deficiency during bacterial infection on the lung, *J. Immunol. 165*, 3934−3940.
23. Khamri, W., Moran, A. P., Worku, M. L., Karim, Q. N., Walker, M. M., Annuk, H., Ferris, J. A., Appelmelk, B. J., Eggleton, P., Reid, K. B., and Thursz, M. R. (2005) Variations in *Helicobacter pylori* lipopolysaccharide to evade the innate immune component surfactant protein D, *Infect. Immun. 73*, 7677−7686.
24. Wu, H., Kuzmenko, A., Wan, S., Schaffer, L., Weiss, A., Fisher, J. H., Kim, K. S., and McCormack, F. X. (2003) Surfactant proteins A and D inhibit the growth of Gram-negative bacteria by increasing membrane permeability, *J. Clin. Invest. 111*, 1589−1602.
25. Khamri, W., Worku, M. L., Anderson, A. E., Walker, M. M., Hawgood, S., Reid, K. B., Clark, H. W., and Thursz, M. R. (2007) *Helicobacter* infection in the surfactant protein D-deficient mouse, *Helicobacter 12*, 112−123.
26. van Rozendaal, B. A., van de Lest, C. H., Van Eijk, M., Van Golde, L. M., Voorhout, W. F., van Helden, H. P., and Haagsman, H. P. (1999) Aerosolized endotoxin is immediately bound by pulmonary surfactant protein D in vivo, *Biochim. Biophys. Acta 1454*, 261−269.
27. Greene, K., Whitsett, J., and Korfhagen, T. (2000) SP-D expression regulates endotoxin mediated lung inflammation in vivo, *Am. J. Respir. Crit. Care Med. 161*, A515.
28. Ikegami, M., Carter, K., Bishop, K., Yadav, A., Masterjohn, E., Brondyk, W., Scheule, R. K., and Whitsett, J. A. (2006) Intratracheal recombinant surfactant protein D prevents endotoxin shock in the newborn preterm lamb, *Am. J. Respir. Crit. Care Med. 173*, 1342−1347.
29. Gardai, S. J., Xiao, Y. Q., Dickinson, M., Nick, J. A., Voelker, D. R., Greene, K. E., and Henson, P. M. (2003) By binding SIRPα or calreticulin/CD91, lung collectins act as dual function surveillance molecules to suppress or enhance inflammation, *Cell 115*, 13−23.
30. Crouch, E. C. (2000) Surfactant protein D and pulmonary host defense, *Respir. Res. 1*, 93−108.
31. Crouch, E., Tu, Y., Briner, D., McDonald, B., Smith, K., Holmskov, U., and Hartshorn, K. (2005) Ligand specificity of human surfactant protein D: Expression of a mutant trimeric collectin that shows enhanced interactions with influenza A virus, *J. Biol. Chem. 280*, 17046−17056.
32. Clark, H., and Reid, K. B. (2002) Structural requirements for SP-D function in vitro and in vivo: Therapeutic potential of recombinant SP-D, *Immunobiology 205*, 619−631.
33. Muller-Loennies, S., Holst, O., and Brade, H. (1994) Chemical structure of the core region of *Escherichia coli* J-5 lipopolysaccharide, *Eur. J. Biochem. 224*, 751−760.
34. Muller-Loennies, S., Holst, O., Lindner, B., and Brade, H. (1999) Isolation and structural analysis of phosphorylated oligosaccharides obtained from *Escherichia coli* J-5 lipopolysaccharide, *Eur. J. Biochem. 260*, 235−249.
35. Muller-Loennies, S., Brade, L., MacKenzie, C. R., Di Padova, F. E., and Brade, H. (2003) Identification of a cross-reactive epitope widely present in lipopolysaccharide from enterobacteria and recognized by the cross-protective monoclonal antibody WN1 222-5, *J. Biol. Chem. 278*, 25618−25627.
36. Brimacombe, J. S., and Kabir, K. M. S. (1986) Convenient synthesis of L-*glycero*-D-*manno*-heptose and D-*glycero*-D-*manno*-heptose, *Carbohydr. Res. 152*, 329−334.
37. Reiter, A., Zamyatina, A., Schindl, H., Hofinger, A., and Kosma, P. (1999) Synthesis of *Pseudomonas aeruginosa* lipopolysaccharide core antigens containing 7-*O*-carbamoyl-L-*glycero*-α-D-*manno*-heptopyranosyl residues, *Carbohydr. Res. 317*, 39−52.
38. Paulsen, H., and Heitmann, A. C. (1988) Synthesis of structures of the inner core region of lipopolysaccharides, *Liebigs Ann. Chem.*, 1061−1071.
39. Guzlek, H., Graziani, A., and Kosma, P. (2005) A short synthesis of D-*glycero*-D-*manno*-heptose 7-phosphate, *Carbohydr. Res. 340*, 2808−2811.
40. Balla, E., Zamyatina, A., Hofinger, A., and Kosma, P. (2007) Synthesis of a deoxy-analogue of ADP L-*glycero*-*β*-D-*manno*-heptose, *Carbohydr. Res.* (in press).
41. Crouch, E. C., Smith, K., McDonald, B., Briner, D., Linders, B., McDonald, J., Holmskov, U., Head, J., and Hartshorn, K. (2006) Species differences in the carbohydrate binding preferences of surfactant protein D, *Am. J. Respir. Cell Mol. Biol. 35*, 84−94.
42. Otwinowski, Z., and Minor, W. (1997) Processing of X-ray diffraction data collected in oscillation mode, *Methods Enzymol. 276*, 307−326.
43. Emsley, P., and Cowtan, K. (2004) Coot: Model-Building Tools for Molecular Graphics, *Acta Crystallogr. D60*, 2126−2132.
44. Kleywegt, G. J. (1995) Dictionaries for heteros, *CCP4/ESF-EACBM Newsletter on Protein Crystallography 31*, 45−50.
45. Kooistra, O., Bedoux, G., Brecker, L., Lindner, B., Sanchez, C. P., Haras, D., and Zahringer, U. (2003) Structure of a highly phosphorylated lipopolysaccharide core in the Delta algC mutants derived from *Pseudomonas aeruginosa* wild-type strains PAO1 (serogroup O5) and PAC1R (serogroup O3), *Carbohydr. Res. 338*, 2667−2677.
46. Choudhury, B., Carlson, R. W., and Goldberg, J. B. (2005) The structure of the lipopolysaccharide from a galU mutant of *Pseudomonas aeruginosa* serogroup-O11, *Carbohydr. Res. 340*, 2761−2772.
47. Sadovskaya, I., Brisson, J. R., Lam, J. S., Richards, J. C., and Altman, E. (1998) Structural elucidation of the lipopolysaccharide core regions of the wild-type strain PAO1 and O-chain-deficient mutant strains AK1401 and AK1012 from *Pseudomonas aeruginosa* serotype O5, *Eur. J. Biochem. 255*, 673−684.
48. Bystrova, O. V., Shashkov, A. S., Kocharova, N. A., Knirel, Y. A., Lindner, B., Zahringer, U., and Pier, G. B. (2002) Structural studies on the core and the O-polysaccharide repeating unit of *Pseudomonas aeruginosa* immunotype 1 lipopolysaccharide, *Eur. J. Biochem. 269*, 2194−2203.
49. Allen, M. J., Laederach, A., Reilly, P. J., Mason, R. J., and Voelker, D. R. (2004) Arg343 in human surfactant protein D governs discrimination between glucose and N-acetylglucosamine ligands, *Glycobiology 14*, 693−700.
50. Leth-Larsen, R., Garred, P., Jensenius, H., Meschi, J., Hartshorn, K., Madsen, J., Tornoe, I., Madsen, H. O., Sorensen, G., Crouch, E., and Holmskov, U. (2005) A common polymorphism in the SFTPD gene influences assembly, function, and concentration of surfactant protein D, *J. Immunol. 174*, 1532−1538.

BI7020553